Immunobiology 224 (2019) 834–842

Contents lists available at ScienceDirect

Immunobiology

journal homepage: www.elsevier.com/locate/imbio

# Factors influencing multinucleated giant cell formation *in vitro*

Kevin L. Trout, Andrij Holian*

*Department of Biomedical and Pharmaceutical Sciences, University of Montana, Missoula, MT, United States*

ARTICLE INFO

*Keywords:*
Multinucleated giant cell
Macrophage
Cell fusion
Cell culture
Mouse

ABSTRACT

Macrophages fuse together to form multinucleated giant cells (MGC) in granulomas associated with various pathological conditions. Improved *in vitro* methods are required to better enable investigations of MGC biology and potential contribution to disease. There is a need for standardization of MGC quantification, purification of MGC populations, and characterization of how cell culture variables influence MGC formation. This study examined solutions to address these needs while providing context with other current and alternative methods. Primary mouse bone marrow-derived macrophages were treated with interleukin-4, a cytokine known to induce fusion into MGC. This model was used to systematically assess the influence of cell stimulant timing, cell seeding density, colony stimulating factors, and culture vessel type. Results indicated that MGC formation is greatly impacted by alterations in certain culture variables. An assessment of previously published research showed that these culture conditions varied widely between different laboratories, which may explain inconsistencies in the literature. A particularly novel and unexpected observation was that MGC formation appears to be greatly increased by silicone, which is a component of a chamber slide system commonly used for MGC studies. The most successful quantification method was fluorescent staining with semi-automated morphological evaluation. The most successful enrichment method was microfiltration. Overall, this study takes steps toward standardizing *in vitro* methods, enhancing replicability, and guiding investigators attempting to culture, quantify, and enrich MGC.

## 1. Introduction

Multinucleated giant cells (MGC) are homotypic macrophage syncytia associated with granulomas. Occasionally, other cell types that become multinucleated in pathological conditions are referred to as giant cells (Trout et al., 2016); however, the focus of this study is on multinucleated cells of monocyte/macrophage origin. These MGC are found in some autoimmune or idiopathic conditions, but are most commonly formed as a result of exposure to persistent foreign microorganisms or materials. Recent *in vitro* studies have led to many new discoveries about MGC, such as their mechanism of formation (Helming and Gordon, 2009). However, many of these studies are completed using a range of methods with little systematic comparison or justification.

Investigators have observed fusion of monocyte/macrophage cells into MGC *in vitro* using primary cells and cell lines from a variety of tissue sources and species. Species include human (McNally and Anderson, 2015), mouse (Jay et al., 2010; Lemaire et al., 2011; Yagi et al., 2007), rat (Lemaire et al., 2011), rabbit (Warfel, 1978), and pig (Tambuyzer and Nouwen, 2005). Primary cells include bone marrow-derived macrophages (BMdM) (Jay et al., 2010; Yagi et al., 2007), blood monocytes (McNally and Anderson, 2015), peritoneal macrophages (Lemaire et al., 2011; Warfel, 1978), alveolar macrophages (Lemaire et al., 2011; Warfel, 1978), splenic macrophages (Yagi et al., 2007), and microglia (Tambuyzer and Nouwen, 2005). Cell lines include RAW264.7 (Jay et al., 2010), UG3 (Ikeda et al., 1998), and J774 (Lemaire et al., 2011). While it is useful to make observations using a variety of model systems, results can be difficult to compare. Cell lines present a unique challenge because multinucleation due to rapid divisions of immortalized cells could lead to artifacts, though they may be particularly useful for studying MGC in the context of cancer. The two most commonly published *in vitro* MGC models are human monocytes and mouse BMdM. There are certain advantages to mouse BMdM: availability of transgenic models, replicability gained from genetic and environmental interindividual similarity, ethical considerations, and ability to obtain high yields of relatively pure monocyte/macrophage

*Abbreviations:* MGC, multinucleated giant cell; BM, bone marrow; BMdM, BM-derived macrophage; IL, interleukin; CSF, colony-stimulating factor; M-CSF, macrophage CSF; GM-CSF, granulocyte-macrophage CSF; RGD, arginylglycylaspartic acid; PS, untreated polystyrene; TCPS, tissue culture-treated polystyrene

* Corresponding author at: Center for Environmental Health Sciences, Department of Biomedical and Pharmaceutical Sciences, University of Montana, 32 Campus Dr, Missoula, MT, 59812, United States.

*E-mail address:* andrij.holian@umontana.edu (A. Holian).

https://doi.org/10.1016/j.imbio.2019.08.002
Received 24 June 2019; Received in revised form 18 July 2019; Accepted 3 August 2019
Available online 10 August 2019

**Table 1**
Methods analysis. Assessment of culture variables during IL-4-induced fusion of mouse BMdM into MGC. All studies used a two-part process: maturation of BM cells using M-CSF (**A**), followed by fusion into MGC using IL-4 (**B**). Notes for specific parameters are indicated by asterisks. *Stimulating proteins were occasionally sourced from cell line supernatants rather than recombinant proteins. **Media was changed periodically throughout culture period. ***%Fusion estimated from BALB/c mice rather than C57Bl/6.

A. Overview and BM maturation

| Laboratory | # of articles | Media | %FBS | Antibiotic | M-CSF, ng/mL | Flt3L, ng/mL | Days |
|---|---|---|---|---|---|---|---|
| Aderem | 1 | DMEM | 10 | Yes | 50 | No | 4 |
| Gordon | 5 | αMEM,RPMI,OptiMEM | 10 | Yes | 50* | No | 3-10 |
| Keegan | 2 | αMEM | 10 | Yes | 20 | No | 1-5 |
| Kyriakides | 6 | IMDM | 10-20 | Yes | 1.5 | 100 | 10** |
| Miyamoto | 6 | αMEM | 10 | No | 50 | No | 2-3 |
| Morrison | 2 | αMEM | 10 | Yes | 30 | No | 2 |
| Park | 1 | DMEM | 10 | No | 10 | No | 7 |

B. MGC formation and quantification

| Laboratory | Cell seeding, x$10^5$/$cm^2$ | Growth surface | IL-4, ng/mL | CSF, ng/mL | Days | Primary quantification | MGC definition | %Fusion estimate |
|---|---|---|---|---|---|---|---|---|
| Aderem | Unspecified | Unspecified | 50 | No | 6 | Ploidy | > 16n ploidy | 8 |
| Gordon | 1.3-2.5 | Permanox | 100* | ± GM 100 | 1-4 | %Fusion | > 2 nuclei | 0-64 |
| Keegan | Unspecified | Glass | 10 | M 20 | 5 | %Fusion | > 2 nuclei | 46*** |
| Kyriakides | 2.6-5.3 | Untreated PS | 10 | ± GM 10 | 3-7** | %Fusion | > 2 nuclei | 29-77 |
| Miyamoto | 1.6 | Microplate | 50 | ± GM 50, other | 2-10 | MGC/well, /$cm^2$ | > 3 nuclei | 0.2-10 |
| Morrison | 0.15 | Microplate | 50 | GM 50 | 4-8 | MGC/view | > 3 nuclei | N/A |
| Park | Unspecified | Permanox | 25 | No | 7 | MGC number | > 1 nucleus | N/A |

primary cell populations using simple methods.

It is common for *in vitro* studies involving BMdM fusion into MGC to first use macrophage colony-stimulating factor (M-CSF) for BM cell maturation, followed by treatment with interleukin (IL)-4 to stimulate MGC formation. Osteoclasts have been formed *in vitro* using similar methods, except that receptor activator of nuclear factor kappa-B ligand (RANKL) is used instead of IL-4. IL-13 signaling has some overlap with IL-4, and both cytokines each result in similar rates of MGC formation (DeFife et al., 1997). Monocytes/macrophages have also been stimulated to fuse into MGC *in vitro* by other means: live microbes, microbial components, concanavalin A with/without interferon-γ in older publications, genetic manipulations, and stimulating factors released from other cells. Some researchers use co-stimulatory factors together with IL-4, the most common of which is granulocyte-macrophage colony-stimulating factor (GM-CSF). One laboratory group (Table 1, Kyriakides) reports quite high fusion with Fms-related tyrosine kinase 3 ligand (Flt3L) when delivered together with IL-4. GM-CSF and Flt3L are often used to generate dendritic cells with phenotypes distinct from each other (Xu et al., 2007, p. 3) and from M-CSF-dependent macrophages (Akagawa et al., 1996; Lacey et al., 2012). MGC are traditionally considered to be more macrophage-like, but some suggest dendritic cells can also fuse (Dong et al., 2011; Oh et al., 2014; Rivollier et al., 2004). Because these cell types have many overlapping features, more studies are needed to examine phenotypes as they relate to MGC.

Experimental models of IL-4-induced BMdM fusion vary widely in terms of *in vitro* conditions, such as media composition, stimulant concentrations, culture timing, and cell seeding density (Table 1). Another important variable is the cell growth surface. These surfaces may include untreated polystyrene (PS), tissue culture-treated PS (TCPS), glass, various biomaterials, or various coatings. MGC formation has been reported to be enhanced on chamber slides made from Permanox™ plastic (Helming and Gordon, 2007). Also, a culture dish coating of particular interest is Arginine-Glycine-Aspartate (RGD) (McNally and Anderson, 2015), which is a tripeptide sequence present in extracellular matrix proteins (*e.g.*fibronectin) that can coat implanted foreign bodies and are bound by integrins for cell attachment.

One of the most widely used MGC quantification metrics is the percent fusion of MGC defined morphologically, usually *via*microscopy, as containing three or more nuclei within a common cytoplasm. Although binucleated cells could be MGC precursors, they could also arise from cells undergoing mitosis without yet completing cytokinesis, so binucleated cells are often excluded from MGC calculations to avoid artifacts that may especially occur in cell line or cancer studies. A fusion index is calculated by dividing the total number of nuclei within MGC by the total nuclei in all cells within the field of view or sample, which can then be converted to a percent. This normalized metric provides a meaningful number that can be used for comparisons between multiple studies, while other limited relative metrics (*i.e.*MGC number per field of view) only allow for comparisons within a single study. The percent fusion metric is also more objective than semi-quantitative scoring. However, counting all the nuclei can be tedious. High content imaging methods have recently been described (Pegoraro et al., 2014), but automated methods may require specialized equipment such as a laser scanning cytometer and can be less accurate when it comes to distinguishing MGC from clumped macrophages.

Enrichment of MGC from mixed cultures would allow for more effective analysis of these cells. Cells with unique surface proteins can be targeted by antibodies for sorting using methods such as magnetic-activated or fluorescence-activated cell sorting (MACS or FACS). Certain surface proteins are upregulated in MGC (*e.g.*dendritic cell–specific transmembrane protein (Yagi et al., 2005)), but whether the magnitude of upregulation is sufficient for effective sorting has not yet been determined. Due to the lack of MGC-specific markers, nuclear fluorescence has been used with flow cytometry to distinguish MGC from macrophages (Dutta et al., 2015; Schlesinger et al., 1984). However, these methods may have undesired effects on subsequent *in vitro* assays due to cell stress during handling and interference from stains or antibodies. Manual isolation methods such as laser capture microdissection (Luttikhuizen et al., 2007) or picking with a micromanipulator (Seitzer et al., 1997; Solari et al., 1995) are damaging to cells and are not feasible for large scale experiments. Some investigators propose that a short incubation with trypsin or other proteases allows mononucleated cells to be removed by washing while multinucleated cells remain (Dickson et al., 2008; Tezuka et al., 1992), but this technique can result in low purity and artificially selects for a phenotype of cells containing more adhesion proteins. Density gradient centrifugation is

suggested to result in partial purification of osteoclasts (Collin-Osdoby and Osdoby, 2012), so testing this method for MGC separation would be valuable. Finally, a simple approach without the need for stains is to sort based on size, which may be possible using differential centrifugation (Xu et al., 2013), microfluidics, microfiltration (Milde et al., 2015), or light scatter signals from flow cytometry.

The objective of this study was to evaluate how these various *in vitro* conditions influence IL-4-induced fusion of primary mouse BMdM into MGC, as well as improve methods for MGC quantification and enrichment. Experimental variables were selected which we hypothesized would have the greatest impact on MGC formation, including treatment timeline, seeding density, CSF treatment, and growth surface. A quantification method was developed using fluorescent staining for a semi-automated approach to morphological evaluation using routine microscope equipment and freely available software. Finally, enrichment methods which we expected to be most promising were tested for sorting MGC based on size or density. Results will help guide investigators attempting to study MGC, enhance replicability, and elucidate factors critical to MGC formation. Furthermore, observations such as fusion kinetics or reactions to different materials/surfaces have implications in understanding granuloma formation in response to foreign materials or biomaterials.

## 2. Methods

### 2.1. Analysis of methods in literature

Primary research involving IL-4-induced fusion of mouse BMdM into MGC was assessed. Related published research methods were grouped according to articles sharing a common author, as shown in each row of Table 1. The “Laboratory” column contains the last name of this author, which is often the senior or corresponding author on the cited publication(s). The articles examined include: Aderem (Sissons et al., 2012), Gordon (Helming et al., 2009, 2008; Helming and Gordon, 2007; Milde et al., 2015; Sheikh et al., 2015), Keegan (Moreno et al., 2007; Yu et al., 2011), Kyriakides (Jay et al., 2010, 2007; MacLauchlan et al., 2009; Moore et al., 2016, 2015; Skokos et al., 2011), Miyamoto (Katsuyama et al., 2015; Miyamoto et al., 2012a,b; Oya et al., 2017; Yagi et al., 2007, 2005), Morrison (Khan et al., 2016, 2013), and Park (Binder et al., 2013). Seeding density during the MGC formation step was calculated to a universal unit of cells/cm$^2$ where possible. The quantification method most widely used in all MGC literature, including *in vivo* studies, is %fusion of MGC defined as containing > 2 nuclei. However, some BMdM publications deviated from this standard. Estimates of %fusion were calculated using data graphs and/or representative images from these publications where possible. Accuracy of these estimates may vary depending on the amount of information provided in the article.

### 2.2. Cell culture materials and methods

Cells were grown in a humidified, water jacketed incubator (Thermo Fisher Scientific, Waltham, MA) at 37 °C and 5% $CO_2$. Sterile 0.2 μm filtered culture media consisted of RPMI-1640 with 10% heat-inactivated fetal bovine serum (FBS), 25 mM HEPES, 2 mM L-glutamine, 1 mM sodium pyruvate, 100 I.U./mL penicillin, and 100 μg/mL streptomycin (FBS: VWR Seradigm, Radnor, PA; all others: Corning subsidiary Mediatech, Manassas, VA). Cells were suspended by using 0.05% trypsin with 0.53 mM EDTA in HBSS (Corning) or Accutase® with 0.5 mM EDTA in Dulbecco’s PBS (BioLegend, San Diego, CA), followed by physical dislodging of cells as necessary using a cell scraper or pipette action. When specified, cells were fixed by 4% paraformaldehyde in PBS for 10 min at room temperature. Treatment concentrations for all recombinant murine proteins was 30 ng/mL, including M-CSF (R&D Systems, Minneapolis, MN), GM-CSF (PeproTech, Rocky Hill, NJ), and IL-4 (R&D Systems). Centrifugations of cells in tubes were performed at $RCF_{avg}$ 300 x *g* for 5 min. Cytocentrifugations of cells onto slides were performed at approximately $RCF_{avg}$ 250 x *g* for 5 min. Cell counting was completed using a Beckman Coulter (Indianapolis, IN) Z2 cell counter.

Permanox is a trademarked (Nalge Nunc International, Rochester, NY) polymethylpentene (TPX RT18XB; Mitsui Chemicals, Tokyo, Japan) tissue culture-treated growth surface. Permanox slides have a silicone gasket (MDX4-4210; Dow Corning, Midland, MI) that connects removable natural polystyrene chamber walls. Media working volumes per chamber or vessel were as follows: 8-chamber permanox slides (Thermo Fisher) at 0.4 mL, 60 x 15 mm permanox dishes (Thermo Fisher) at 5 mL, 8-chamber borosilicate glass slides with non-removable wells (Thermo Fisher) at 0.4 mL, 24-well PS or TCPS plates (Greiner Bio-One, Monroe, NC) at 0.5 mL, and T75 TCPS flasks at 20 mL. Designated plates were coated with 5 μg/cm$^2$ RGD protein polymer (F5022; Sigma-Aldrich, St. Louis, MO) for 30 min, then washed twice with PBS and used immediately.

### 2.3. Mice

Male and female C57Bl/6 mice (Jackson Laboratories, Bar Harbor, ME) aged 9–20 weeks were used for all experiments. Mice were housed in microisolator cages with *ad libitum* access to food and water in a specific-pathogen-free facility maintained at 22 ± 2 °C, 30–40% humidity, and 12-h light/12-h dark cycle. Mice were euthanized by intraperitoneal injection of sodium pentobarbital followed by a secondary mechanical means of euthanasia prior to removal of rear legs for bone marrow isolation in a tissue culture hood. Experimental protocols were approved by the University of Montana Institutional Animal Care and Use Committee.

### 2.4. Multinucleated giant cell (MGC) culture

BMdM methods were similar to those previously used in our laboratory (Migliaccio et al., 2008). BM was flushed from the tibiae and femora in a sterile environment, pooled, centrifuged, resuspended in media, and seeded at 4 × 10$^5$ cells/cm$^2$ in a T75 flask. Cells were incubated at 37 °C overnight. Adherent stromal cells were discarded, and suspended macrophage progenitor cells were collected. In culture timeline evaluation experiments, these suspended progenitor cells were seeded at 6 × 10$^5$ cells/cm$^2$ in Permanox slides with M-CSF until the media was replaced with IL-4-containing media at varying time points (Fig. 2). In other experiments after the timeline was optimized, suspended progenitor cells were added to T75 flasks at 2 × 10$^5$ cells/cm$^2$ with M-CSF for four days to mature into BMdM. Then, mature BMdM were seeded at 9 × 10$^5$ cells/cm$^2$ (established in Fig. 3) in specified culture vessels with IL-4 for four days.

### 2.5. Staining and microscopy

Cells in initial experiments (Fig. 1A, B) were stained using a method similar to Wright-Giemsa (PROTOCOL™ Hema 3™; Fisher Scientific, Kalamazoo, MI) by submerging slides in a methanol-based fixative for 90 s, “Solution I” for 120 s, “Solution II” for 30 s, and water for 90 s. Cells in remaining experiments were stained with HCS NuclearMask Blue followed by CellMask Orange Plasma Membrane according to manufacturer (Thermo Fisher) recommendations. When necessary, FluorSave™ (Calbiochem, MilliporeSigma, Burlington, MA) medium was used to mount coverslips on slides. Images for MGC quantification were collected using a routine transmitted light and epifluorescent Zeiss Axioskop upright microscope with AxioCamMR3 camera (Carl Zeiss, Jena, Germany) at 200x magnification with DAPI and TRITC filters. At least five random, independent (non-overlapping) images were acquired per sample chamber. Fluorescent images used to illustrate differences among staining methods (Fig. 1C, D) were collected using an Olympus FluoView FV1000 IX81 confocal microscope.

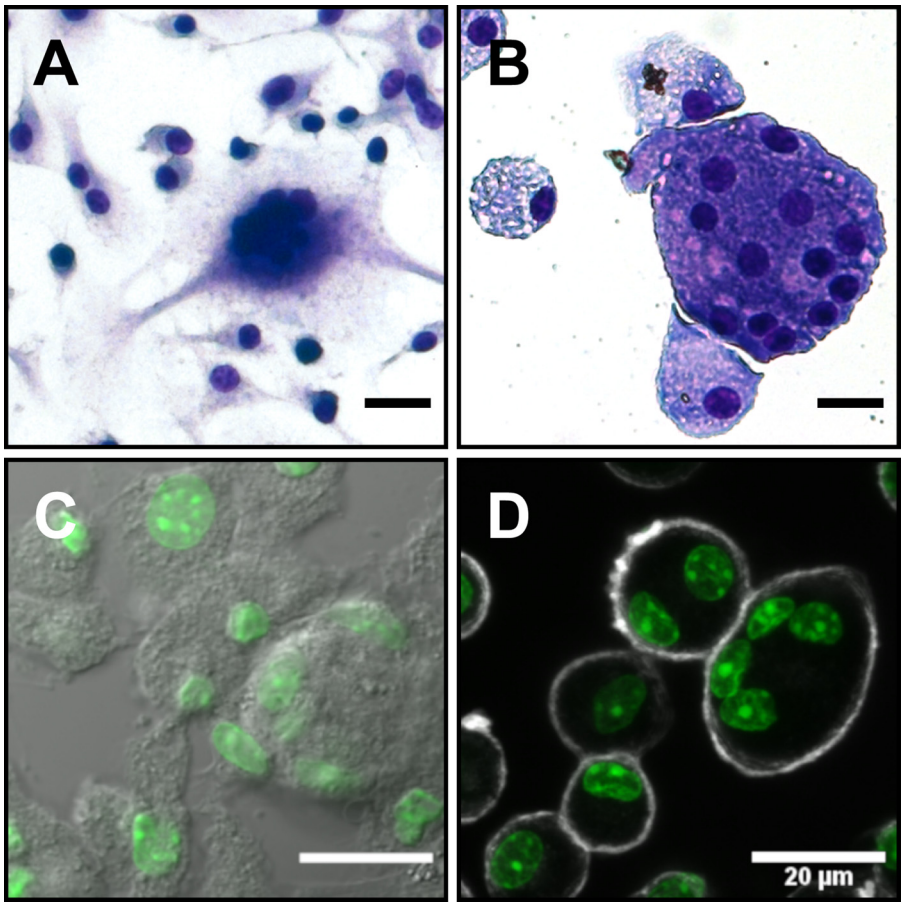


**Fig. 1.** Quantification method. Comparison of staining methods for morphological quantification of MGC. Brightfield images show cells stained with Hema 3, a method similar to Wright-Giemsa. Pseudo-color fluorescent images show cells stained with NuclearMask (green) and a second channel consisting of either differential interference contrast (DIC) or CellMask Plasma Membrane stain. (A) Example of lower-quality staining with adherent cells. (B) Example of higher-quality staining with cytocentrifuged cells. (C) NuclearMask + DIC. (D) NuclearMask + CellMask. Scale bars 20 µm.

### 2.6. Quantification

MGC were defined morphologically as containing three or more nuclei within a common cytoplasm. The number of MGC nuclei were manually counted, while the total nuclei were counted by an automated method developed in the freely available, open-source ImageJ v1.51-1.52 software (https://imagej.nih.gov/ij/index.html) as shown in Video S1. The number of nuclei within MGC was divided by total nuclei within all cells to calculate a fusion index for each image field. Fusion indices of all image fields within a sample were combined into a mean, then multiplied by 100 to be expressed as percent fusion.

### 2.7. Enrichment

Cultures of mature mouse BMdM treated with IL-4, as described above, contain a mixture of MGC and macrophages. Separation of this cell mixture into purified populations was attempted using three enrichment methods. First, the mixed cell suspension was layered on sterile isotonic Percoll™ colloid (GE Healthcare, Uppsala, Sweden) diluted with cell culture medium to densities of 1.02, 1.05, and 1.08 g/mL to form a discontinuous gradient. The gradient was centrifuged at $RCF_{avg}$ 400 x *g* for 30 min in a swinging bucket rotor with slow acceleration/deceleration. Fractions were collected with a sterile Pasteur pipette at gradient interfaces for staining and analysis. Second, the mixture of cells was stained with NuclearMask for measuring nuclear fluorescence, forward scatter (FSC), and side scatter (SSC) with an Attune NXT flow cytometer (Thermo Fisher). Third, the mixture of cells was suspended in 2 mL media, transferred onto a pre-rinsed cell strainer (PluriStrainer by PluriSelect; Leipzig, Germany), and washed twice with 4 mL/wash into a tube. Then, the strainer was inverted and washed twice with 4 mL/wash into a new tube. The first tube contained cells that were small enough to pass through the sieve, while the other tube contained larger cells that were blocked by the sieve. The number of MGC relative to macrophages in each tube was assessed for various cell strainer sizes.

### 2.8. Statistics

Graphs display mean and standard error for $n \geq 3$ independent replicate mice in each condition. M-CSF groups in culture timing experiments were analyzed by linear regression to assist interpretation of MGC formation over time (Fig. 2). Effects of CSF on IL-4-induced fusion was assessed by one-way ANOVA (Fig. 4). Fusion data from cell seeding density (Fig. 3) and culture vessel (Fig. 5) experiments included some sample groups with a normal underlying distribution and some groups with a nonsymmetric, bimodal distribution due to the large number of zero values. This was confirmed by Shapiro-Wilk tests. This violates assumptions of normality required by parametric methods and violates assumptions that all sample distributions are approximately the same form required by the nonparametric Kruskal-Wallis test. Therefore, a one-sample sign-test with one-sided alternative was selected to determine whether % fusion of each group was significantly different from zero. The Holm-Bonferroni correction was applied to p-values to counteract increased type I error due to multiple comparisons. All analysis was completed in R v3.4.0 statistical software. Statistical significance was defined as a probability of type I error occurring at less than 5%.

## 3. Results

### 3.1. Analysis of methods in literature

Primary literature was systematically assessed to determine which culture variables may have the most potential to influence IL-4-induced

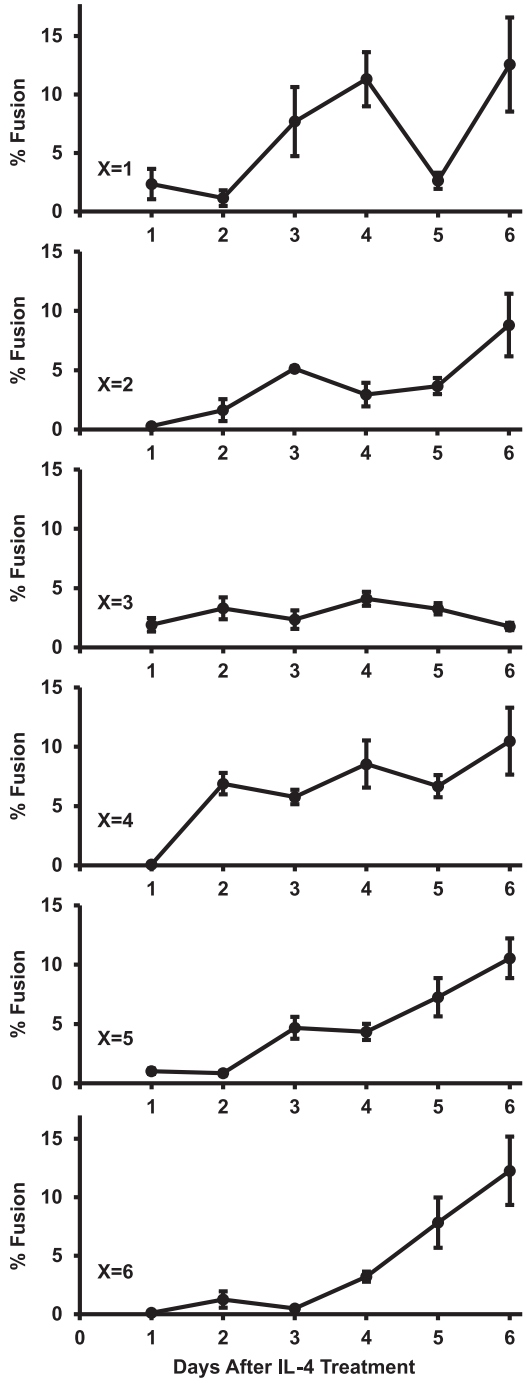


**Fig. 2.** Culture timing effects on MGC formation. Time-course examining fusion kinetics of immature and mature BMdM. BM on Permanox slides were treated with M-CSF for x days until media was replaced with IL-4-containing media. Then, groups of cells were fixed daily for 6 days to be analyzed for % fusion. Regression lines with y-intercepts set to zero had slopes of 1.8, 1.2, 0.6, 1.8, 1.5, and 1.4 corresponding to groups x = 1, 2, 3, 4, 5, and 6 (regression not displayed on graphs). Higher slopes reflect fast and consistent increases in % fusion.

fusion of mouse BMdM into MGC (Table 1). Most studies used BM from C57Bl/6 mice ranging in age from 4 (Keegan) to 30 weeks (Gordon). Mouse sex, BM growth surface, and seeding density during the BM maturation step were rarely reported. Methods for elimination of stromal cells widely varied or were not reported. Determining correlations between culture variables and effects on fusion was difficult because the methods were so widely varied. However, this literature

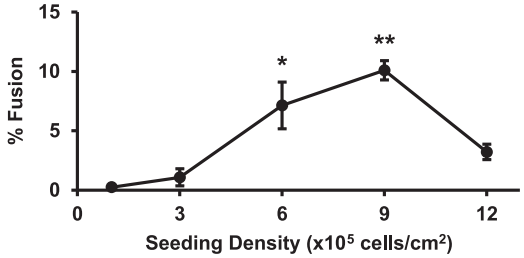


**Fig. 3.** Cell seeding density effects on MGC formation. BMdM were added to Permanox slides at the specified seeding density and treated with IL-4. After four days, cells were analyzed for % fusion. Samples with % fusion significantly greater than zero by one-sample sign-test are shown as *$p < 0.05$ and **$p < 0.01$.

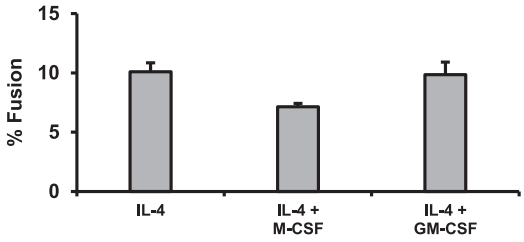


**Fig. 4.** Colony stimulating factor effects on MGC formation. BMdM were added to Permanox slides at $9 \times 10^5$ cells/cm$^2$ and treated with IL-4 alone or in combination with M-CSF or GM-CSF. After four days, cells were analyzed for % fusion. No significant effects were observed by one-way ANOVA at $p < 0.05$ level.

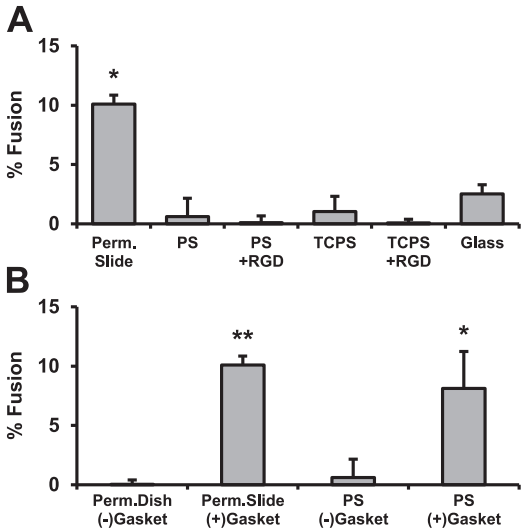


**Fig. 5.** Culture vessel effects on MGC formation. BMdM were added to the specified culture vessels at $9 \times 10^5$ cells/cm$^2$ and treated with IL-4. After four days, cells were analyzed for % fusion. (A) Culture vessels included Permanox chamber slides, glass, untreated polystyrene (PS), tissue culture-treated PS (TCPS), and RGD-treated PS or TCPS. The Permanox slides are manufactured with chambers attached *via* silicone gasket, which was hypothesized to be causing increased MGC formation. (B) Therefore, fusion was compared for cells on Permanox dishes without gaskets, Permanox slides containing gaskets, PS wells without gaskets, and PS wells containing gasket pieces cut from the slides. Samples with % fusion significantly greater than zero by one-sample sign-test are shown as *$p < 0.05$ and **$p < 0.01$.

synthesis demonstrates the importance of investigating these variables because results show a very broad range of % fusion outcomes.

### 3.2. Quantification method

Non-standard MGC quantification methods in the literature create challenges when attempting to compare and evaluate results. The normalized and most objective metric is the percent fusion of macrophages into MGC, which are defined morphologically as containing three or more nuclei within a common cytoplasm. These cells are typically visualized using brightfield microscopy with traditional histological stains, but manually counting nuclei to calculate %fusion is tedious and impractical for larger scale studies. Faster, more automated analysis methods are possible by segmenting, or partitioning, images into regions representing nuclei and cell borders. However, segmentation of these images was challenging due to inconsistencies in staining quality (Fig. 1A, B) that often resulted in poor contrast and unclear distinctions between nuclei, cytoplasm, and cell borders. Also, MGC cytoplasm tended to stain darker than macrophage cytoplasm, which obscured MGC nuclei during counting.

In an attempt to improve image segmentation based on nuclei, a fluorescent nuclear stain was used together with differential interference contrast (DIC; Fig. 1C). This method allowed for automated counting of nuclei, but cell borders in the DIC channel were unclear in regions where other cells were within close proximity. Therefore, a plasma membrane stain was added to improve visualization of cell outlines and more accurately determine whether a particular nucleus was within a macrophage or MGC (Fig. 1D). The resulting images were well-suited for semi-automated analysis with freely available software (ImageJ) to calculate % fusion. Furthermore, this stain combination is compatible with routine fluorescent microscopes, which promoted simple, rapid acquisition of images in subsequent experiments.

### 3.3. Culture timing

Primary mouse bone marrow cells treated with macrophage colony-stimulating factor (M-CSF) mature into bone marrow-derived macrophages (BMdM), which then fuse into MGC when treated with interleukin-4 (IL-4). An evaluation of studies using this *in vitro* model shows that various permutations of culture conditions can have a range of effects on BMdM fusion outcomes (Table 1). In order to make a more systematic assessment of these variables, we first compared cell stimulation timelines to determine kinetics of MGC formation and effects of BMdM maturity on percent fusion.

As expected, BM cells that received M-CSF for only one day (x = 1) were immature compared to cells in extended cultures. The average total number of nuclei per image field on the first day after IL-4 treatment was 157 for the x = 1 group, while all other groups were 286 ± 19 (standard error). Although the total number of nuclei in this group remained consistent throughout all IL-4 treatment durations (range 132 to 157), the rates of fusion were highly variable (Fig. 2, x = 1). This suggests MGC death, detachment, or splitting may have been occurring. Many of these MGC had a morphology that was different from those generated from mature BMdM *in vitro* or the MGC that are typically observed *in vivo*. They appeared in localized regions of the culture and often consisted of vast cytoplasm containing clustered areas of packed nuclei.

More consistent MGC results were observed with mature BMdM (Fig. 2). In all cases, at least two days with IL-4 was required for high levels of MGC. A relatively early timepoint with consistently high fusion (M-CSF for 4d, then IL-4 for 4d) was selected for subsequent experiments. The shorter culture period allows for more rapid sequential experiments while still having sufficient number of MGC and avoiding unexpected effects on primary cell condition when they are maintained in culture for extended periods of time.

### 3.4. Cell seeding density

The next *in vitro* variable examined was mouse BMdM seeding density prior to IL-4-induced fusion into MGC. High cell density resulted in high fusion, which peaked at $9 \times 10^5$ cells/cm$^2$ (Fig. 3). Fusion was reduced in the highest seeding density, $12 \times 10^5$ cells/cm$^2$. This culture contained overlapping/clumping cells. Likely, MGC formation was reduced due to the number of cells exceeding available space for attachment to the growth surface. Therefore, the seeding density with consistently high fusion, $9 \times 10^5$ cells/cm$^2$, was used for subsequent experiments.

### 3.5. Colony stimulating factors

As in previous experiments, BM cells were differentiated M-CSF. Then, the BMdM were treated with IL-4 alone or in combination with M-CSF or GM-CSF to examine the potential influence on fusion into MGC. Results show that neither CSF significantly alters IL-4-induced fusion (Fig. 4).

### 3.6. Culture vessel

The final *in vitro* variable examined was the influence of common culture vessels on MGC formation. IL-4-induced fusion was highest on Permanox chamber slides (Fig. 5A). MGC were observed in small numbers on all other surfaces: glass, untreated polystyrene (PS) plates, tissue culture-treated PS (TCPS) plates, and RGD-treated PS or TCPS.

Next, we investigated whether increased MGC formation on Permanox slides was a result of the plastic surface (polymethylpentene) or another component of the chamber slide system, particularly the silicone gasket used by the manufacturer to attach the media chamber to the slide base. Cells cultured on intact Permanox slides containing gaskets were compared to cells on round 60 x 15 mm Permanox dishes that did not contain gaskets. As an additional control, cells grown in PS wells were compared to cells in PS wells containing pieces of gasket that were cut from disassembled Permanox chamber slides.

In both cases, significant MGC formation was only observed in the presence of the silicone gasket (Fig. 5B). Similar results were observed in the presence of an alternative piece of silicone (ring gasket from a cryogenic vial; data not shown). This shows that presence of silicone in the culture has a greater influence on MGC formation than the growth surface itself.

### 3.7. Enrichment

Exploratory experiments were completed to enrich MGC from mixed macrophage-MGC cultures. A pre-formed, discontinuous density centrifugation did not provide distinct separation between macrophages and MGC. This indicates that the buoyant densities of these cells are similar, likely as a result of similar ratios of nuclei to cytoplasm. The similar ratios suggest that cytoplasm is conserved during macrophage fusion. More extensive studies are needed to further test this hypothesis, such as continuous density gradients and live cell imaging.

When cell nuclei were fluorescently stained for analysis by flow cytometry, the cells could be distinguished into groups of mononucleated macrophages, binucleated macrophages, and MGC. However, the stain may interfere with experiments requiring cells to be cultured after sorting, so forward scatter (FSC) and side scatter (SSC) parameters were considered as a potential stain-free method of discrimination. MGC tended toward slightly higher FSC and SSC than macrophages, but the overlap in the populations would prevent sufficient separation of highly pure MGC without losing many cells (Fig. S1).

The best enrichment was achieved using microfiltration. Sieve mesh sizes 10, 15, 20, 30, and 35 μm were tested. The enriched population from the 20 μm size had the highest average purity (number of MGC divided by total cells), which was over 20-fold purer than the average

filtrate population. Enrichment efficiency would likely be further increased by protocol optimization (*i.e.*adjusting filter washing procedures) or by using microfiltration in combination with another purification method. This simple approach would be useful for future studies, allowing MGC populations to be compared with macrophage control groups derived from the same source culture while avoiding potential interference from cell stains or cell stress due to extensive handling.

## 4. Discussion

This study shows IL-4-induced fusion into MGC *in vitro* is greatly impacted by alterations in certain culture conditions. This was demonstrated by systematic assessment of cell stimulant timing, cell seeding density, colony stimulating factors, and culture vessel type. A particularly novel discovery is that MGC formation appears to be greatly increased by silicone. MGC culture methods vary widely between different research laboratories, creating challenges when critically comparing results in the literature. Another challenge for researchers attempting to study MGC is the ability to obtain relatively pure populations of these cells together with appropriate macrophage control populations. Solutions to this enrichment problem were explored, with microfiltration emerging as a successful method. Finally, this study was enabled by our improved quantification methods, which provided the means for accurate and efficient analysis of MGC formation.

Morphological analysis to calculate %fusion using brightfield microscopy and traditional histological stains was less suitable for large scale studies, varied in accuracy with stain quality, and became more subjective when cells are densely packed together. Image segmentation was facilitated by using fluorescent nuclear and cell membrane stains, which was more conducive to automation. Quantification could be completed using routine laboratory microscopes and freely available image analysis software, such as ImageJ or CellProfiler. This stain combination would be adaptable to high-throughput automation as necessary. When attempting to distinguish MGC from clumped macrophages, a stain specific for plasma membranes was more effective than stains that diffuse throughout the entire cell. The CellMask plasma membrane stain usually yielded well-defined cell outlines but is not compatible with experiments requiring permeabilization. Alternatives may include lipid, cholesterol, protein, or other novel membrane stains (Wang et al., 2015).

BMdM cell maturity and culture density were important variables affecting fusion. IL-4 treatment of more mature BMdM (at least four days with M-CSF) resulted in more consistent MGC formation than immature BMdM. High cell seeding densities resulted in high % fusion, which is in agreement with previous results by Moreno et al (Moreno et al., 2007) and follows logically with the idea that cells are more likely to fuse when less migration is required to reach proximity. These culture parameters were used for subsequent experiments. No significant difference in fusion was observed when mature BMdM were treated with IL-4 + M-CSF *versus*IL-4 + GM-CSF, which has also been shown by Yagi et al (Yagi et al., 2007). To our knowledge, our report is the first to compare fusion of mature BMdM treated with IL-4-only *versus*CSF co-treatment. No differences were observed, likely because BM were already sufficiently differentiated and cultured at a density optimal for MGC formation. If IL-4 was added to immature BM at a lower culture density, we would hypothesize CSF co-treatment to increase fusion as an indirect side effect of CSF-stimulated proliferation and differentiation.

IL-4-induced fusion of BMdM grown on Permanox slides was over twice as high compared to other culture dishes, including: PS, TCPS, glass, and RGD-modified polystyrene. This was expected based on previous studies with mouse thioglycolate-elicited peritoneal macrophages (Faust et al., 2017; Helming and Gordon, 2007). However, previous reports have not included control experiments to determine which component of the Permanox slide system causes increased fusion. Surprisingly, we found that this occurred due to the presence of a silicone gasket that attaches the media chamber to the slide, rather than the Permanox surface itself. Future studies are needed to determine how cellular events related to macrophage fusion are impacted by silicone. It is possible that culture medium composition or surface properties are altered as a result of adsorption, leachables, or release of by-products from manufacturing or degradation. Clinically, MGC are commonly found surrounding breast implants and in other silicone granulomas (Institute of Medicine, 1999). Understanding these mechanisms are important because of the variety of implantable silicone medical devices with prolonged tissue contact, including those with applications in ophthalmology, otology, cardiology, gastroenterology, orthopedics, and aesthetics.

Many of the culture variables found to be important during fusion of BMdM would likely influence other *in vitro* MGC models as well. For example, we hypothesize that treatment timing and seeding density would also affect fusion in human blood monocyte cultures, which is another frequently published MGC model. Other variables such as CSF treatment effects may differ, as these monocytes are often supplemented with autologous serum instead of additional M-CSF stimulation (McNally and Anderson, 2015). It would be valuable to repeat methods used in this study with other cell models, particularly the experiments examining effects of silicone on MGC formation. Additionally, other future investigations should compare phenotype and function of MGC from various monocyte/macrophage sources, including MGC that have formed *in vivo*. Standardization of *in vitro* methods will facilitate these comparisons. However, isolating large quantities of MGC for *ex vivo* experiments remains challenging, and different methods used to induce MGC formation *in vivo* may result in diverse phenotypes.

Overall, this study demonstrates macrophage fusion is influenced by many experimental variables, which need to be considered to improve *in vitro* study replicability within a laboratory or between different laboratories. It is important for authors to provide detailed methods in publications, such as culture vessel type and cell seeding density. Including an IL-4-only positive control is helpful for interlaboratory comparisons, reduction of false negatives, and troubleshooting when % fusion is outside the typical range. Although we have assessed many major factors affecting MGC formation, there are other possible variables that could be influential. Some examples include hormone variability between serum lots, serum source (Vignery et al., 1990), stimulating factor source, endotoxin levels (Katsuyama et al., 2015), microbial contamination (Gharun et al., 2017), and interindividual differences among organisms used for primary cell collection. This study provides a step toward standardization of major parameters influencing macrophage fusion, and we hope it will serve as a guide for new investigators attempting to culture, quantify, and enrich MGC.

## Declaration of Competing Interest

The authors declare that they have no conflicts of interest.

## Acknowledgements

Samantha Couture (Summer Undergraduate Research Program) helped gather preliminary data that contributed to early development of this project. Technical laboratory support was provided by Center for Environmental Health Sciences core facilities and staff: Lou Herritt, Molecular Histology and Fluorescence Imaging; Pam Shaw, Fluorescence Cytometry. Research funding was provided by an Institutional Development Award (IDeA) from the National Institute of General Medical Sciences (NIGMS) of the National Institutes of Health (NIH) under grant number P30GM103338. Contents of this publication are solely the responsibility of the authors and do not necessarily represent the official views of NIGMS or NIH.

## Appendix A. Supplementary data

Supplementary material related to this article can be found, in the online version, at doi:https://doi.org/10.1016/j.imbio.2019.08.002.

## References


Akagawa, K.S., Takasuka, N., Nozaki, Y., Komuro, I., Azuma, M., Ueda, M., Naito, M., Takahashi, K., 1996. Generation of CD1 + RelB + dendritic cells and tartrate-resistant acid phosphatase-positive osteoclast-like multinucleated giant cells from human monocytes. Blood 88, 4029–4039.

Binder, F., Hayakawa, M., Choo, M.-K., Sano, Y., Park, J.M., 2013. Interleukin-4-induced β-catenin regulates the conversion of macrophages to multinucleated giant cells. Mol. Immunol. 54, 157–163. https://doi.org/10.1016/j.molimm.2012.12.004.

Collin-Osdoby, P., Osdoby, P., 2012. Isolation and culture of primary chicken osteoclasts. In: Helfrich, M.H., Ralston, S.H. (Eds.), Bone Research Protocols, Methods in Molecular Biology. Humana Press, Totowa, NJ, pp. 119–143. https://doi.org/10.1007/978-1-61779-415-5_9.

DeFife, K.M., Jenney, C.R., McNally, A.K., Colton, E., Anderson, J.M., 1997. Interleukin-13 induces human monocyte/macrophage fusion and macrophage mannose receptor expression. J. Immunol. 158, 3385–3390.

Dickson, B.C., Li, S.-Q., Wunder, J.S., Ferguson, P.C., Eslami, B., Werier, J.A., Turcotte, R.E., Kandel, R.A., 2008. Giant cell tumor of bone express p63. Mod. Pathol. 21, 369–375. https://doi.org/10.1038/modpathol.2008.29.

Dong, R., Moulding, D., Himoudi, N., Adams, S., Bouma, G., Eddaoudi, A., Basu, B.P., Derniame, S., Chana, P., Duncan, A., Anderson, J., 2011. Cells with dendritic cell morphology and immunophenotype, binuclear morphology, and immunosuppressive function in dendritic cell cultures. Cell. Immunol. 272, 1–10. https://doi.org/10.1016/j.cellimm.2011.09.012.

Dutta, D.K., Potnis, P.A., Rhodes, K., Wood, S.C., 2015. Wear particles derived from metal hip implants induce the generation of multinucleated giant cells in a 3-dimensional peripheral tissue-equivalent model. PLoS One 10, e0124389. https://doi.org/10.1371/journal.pone.0124389.

Faust, J.J., Christenson, W., Doudrick, K., Ros, R., Ugarova, T.P., 2017. Development of fusogenic glass surfaces that impart spatiotemporal control over macrophage fusion: direct visualization of multinucleated giant cell formation. Biomaterials 128, 160–171. https://doi.org/10.1016/j.biomaterials.2017.02.031.

Gharun, K., Senges, J., Seidl, M., Lösslein, A., Kolter, J., Lohrmann, F., Fliegauf, M., Elgizouli, M., Vavra, M., Schachtrup, K., Illert, A.L., Gilleron, M., Kirschning, C.J., Triantafyllopoulou, A., Henneke, P., 2017. Mycobacteria exploit nitric oxide-induced transformation of macrophages into permissive giant cells. EMBO Rep. 18, 2144–2159. https://doi.org/10.15252/embr.201744121.

Helming, L., Gordon, S., 2009. Molecular mediators of macrophage fusion. Trends Cell Biol. 19, 514–522. https://doi.org/10.1016/j.tcb.2009.07.005.

Helming, L., Gordon, S., 2007. Macrophage fusion induced by IL-4 alternative activation is a multistage process involving multiple target molecules. Eur. J. Immunol. 37, 33–42. https://doi.org/10.1002/eji.200636788.

Helming, L., Tomasello, E., Kyriakides, T.R., Martinez, F.O., Takai, T., Gordon, S., Vivier, E., 2008. Essential role of DAP12 signaling in macrophage programming into a fusion-competent state. Sci. Signal. 1, ra11. https://doi.org/10.1126/scisignal.1159665.

Helming, L., Winter, J., Gordon, S., 2009. The scavenger receptor CD36 plays a role in cytokine-induced macrophage fusion. J. Cell. Sci. 122, 453–459. https://doi.org/10.1242/jcs.037200.

Ikeda, T., Ikeda, K., Sasaki, K., Kawakami, K., Hatake, K., Kaji, Y., Norimatsu, H., Harada, M., Takahara, J., 1998. IL-13 as well as IL-4 induces monocytes/macrophages and a monoblastic cell line (UG3) to differentiate into multinucleated giant cells in the presence of M-CSF. Biochem. Biophys. Res. Commun. 253, 265–272. https://doi.org/10.1006/bbrc.1998.9702.

Institute of Medicine, 1999. Immunology of silicone. In: Bondurant, S., Ernster, V., Herdman, R. (Eds.), Safety of Silicone Breast Implants. National Academies Press, Washington, DC. https://doi.org/10.17226/9602.

Jay, S.M., Skokos, E., Laiwalla, F., Krady, M.-M., Kyriakides, T.R., 2007. Foreign body giant cell formation is preceded by lamellipodia formation and can be attenuated by inhibition of Rac1 activation. Am. J. Pathol. 171, 632–640. https://doi.org/10.2353/ajpath.2007.061213.

Jay, S.M., Skokos, E.A., Zeng, J., Knox, K., Kyriakides, T.R., 2010. Macrophage fusion leading to foreign body giant cell formation persists under phagocytic stimulation by microspheres in vitro and in vivo in mouse models. J. Biomed. Mater. Res. A. 93A, 189–199. https://doi.org/10.1002/jbm.a.32513.

Khan, U.A., Hashimi, S.M., Bakr, M.M., Forwood, M.R., Morrison, N.A., 2016. CCL2 and CCR2 are essential for the formation of osteoclasts and foreign body giant cells. J. Cell. Biochem. 117, 382–389. https://doi.org/10.1002/jcb.25282.

Katsuyama, E., Miyamoto, H., Kobayashi, T., Sato, Y., Hao, W., Kanagawa, H., Fujie, A., Tando, T., Watanabe, R., Morita, M., Miyamoto, K., Niki, Y., Morioka, H., Matsumoto, M., Toyama, Y., Miyamoto, T., 2015. Interleukin-1 receptor-associated kinase-4 (IRAK4) promotes inflammatory osteolysis by activating osteoclasts and inhibiting formation of foreign body giant cells. J. Biol. Chem. 290, 716–726. https://doi.org/10.1074/jbc.M114.568360.

Khan, U.A., Hashimi, S.M., Bakr, M.M., Forwood, M.R., Morrison, N.A., 2013. Foreign body giant cells and osteoclasts are TRAP positive, have podosome-belts and both require OC-STAMP for cell fusion. J. Cell. Biochem. 114, 1772–1778. https://doi.org/10.1002/jcb.24518.

Lacey, D.C., Achuthan, A., Fleetwood, A.J., Dinh, H., Roiniotis, J., Scholz, G.M., Chang, M.W., Beckman, S.K., Cook, A.D., Hamilton, J.A., 2012. Defining GM-CSF– and macrophage-CSF–dependent macrophage responses by in vitro models. J. Immunol. 188, 5752–5765. https://doi.org/10.4049/jimmunol.1103426.

Lemaire, I., Falzoni, S., Zhang, B., Pellegatti, P., Virgilio, F.D., 2011. The P2X7 receptor and Pannexin-1 are both required for the promotion of multinucleated macrophages by the inflammatory cytokine GM-CSF. J. Immunol. 187, 3878–3887. https://doi.org/10.4049/jimmunol.1002780.

Luttikhuizen, D.T., Dankers, P.Y.W., Harmsen, M.C., van Luyn, M.J.A., 2007. Material dependent differences in inflammatory gene expression by giant cells during the foreign body reaction. J. Biomed. Mater. Res. A 83A, 879–886. https://doi.org/10.1002/jbm.a.31420.

MacLauchlan, S., Skokos, E.A., Meznarich, N., Zhu, D.H., Raoof, S., Shipley, J.M., Senior, R.M., Bornstein, P., Kyriakides, T.R., 2009. Macrophage fusion, giant cell formation, and the foreign body response require matrix metalloproteinase 9. J. Leukoc. Biol. 85, 617–626. https://doi.org/10.1189/jlb.1008588.

McNally, A.K., Anderson, J.M., 2015. Phenotypic expression in human monocyte-derived interleukin-4-induced foreign body giant cells and macrophages in vitro: dependence on material surface properties. J. Biomed. Mater. Res. A 103A, 1380–1390. https://doi.org/10.1002/jbm.a.35280.

Migliaccio, C.T., Buford, M.C., Jessop, F., Holian, A., 2008. The IL-4Rα pathway in macrophages and its potential role in silica-induced pulmonary fibrosis. J. Leukoc. Biol. 83, 630–639. https://doi.org/10.1189/jlb.0807533.

Milde, R., Ritter, J., Tennent, G.A., Loesch, A., Martinez, F.O., Gordon, S., Pepys, M.B., Verschoor, A., Helming, L., 2015. Multinucleated giant cells are specialized for complement-mediated phagocytosis and large target destruction. Cell Rep. 13, 1937–1948. https://doi.org/10.1016/j.celrep.2015.10.065.

Miyamoto, H., Katsuyama, E., Miyauchi, Y., Hoshi, H., Miyamoto, K., Sato, Y., Kobayashi, T., Iwasaki, R., Yoshida, S., Mori, T., Kanagawa, H., Fujie, A., Hao, W., Morioka, H., Matsumoto, M., Toyama, Y., Miyamoto, T., 2012a. An essential role for STAT6-STAT1 protein signaling in promoting macrophage cell-cell fusion. J. Biol. Chem. 287, 32479–32484. https://doi.org/10.1074/jbc.M112.358226.

Miyamoto, H., Suzuki, T., Miyauchi, Y., Iwasaki, R., Kobayashi, T., Sato, Y., Miyamoto, K., Hoshi, H., Hashimoto, K., Yoshida, S., Hao, W., Mori, T., Kanagawa, H., Katsuyama, E., Fujie, A., Morioka, H., Matsumoto, M., Chiba, K., Takeya, M., Toyama, Y., Miyamoto, T., 2012b. Osteoclast stimulatory transmembrane protein and dendritic cell–specific transmembrane protein cooperatively modulate cell–cell fusion to form osteoclasts and foreign body giant cells. J. Bone Miner. Res. 27, 1289–1297. https://doi.org/10.1002/jbmr.1575.

Moore, L.B., Sawyer, A.J., Charokopos, A., Skokos, E.A., Kyriakides, T.R., 2015. Loss of monocyte chemoattractant protein-1 alters macrophage polarization and reduces NFκB activation in the foreign body response. Acta Biomater. 11, 37–47. https://doi.org/10.1016/j.actbio.2014.09.022.

Moore, L.B., Sawyer, A.J., Saucier-Sawyer, J., Saltzman, W.M., Kyriakides, T.R., 2016. Nanoparticle delivery of miR-223 to attenuate macrophage fusion. Biomaterials 89, 127–135. https://doi.org/10.1016/j.biomaterials.2016.02.036.

Moreno, J.L., Mikhailenko, I., Tondravi, M.M., Keegan, A.D., 2007. IL-4 promotes the formation of multinucleated giant cells from macrophage precursors by a STAT6-dependent, homotypic mechanism: contribution of E-cadherin. J. Leukoc. Biol. 82, 1542–1553. https://doi.org/10.1189/jlb.0107058.

Oh, Y., Oh, I., Morimoto, J., Uede, T., Morimoto, A., 2014. Osteopontin has a crucial role in osteoclast-like multinucleated giant cell formation. J. Cell. Biochem. 115, 585–595. https://doi.org/10.1002/jcb.24695.

Oya, A., Katsuyama, E., Morita, M., Sato, Y., Kobayashi, T., Miyamoto, K., Nishiwaki, T., Funayama, A., Fujita, Y., Kobayashi, T., Matsumoto, M., Nakamura, M., Kanaji, A., Miyamoto, T., 2017. Tumor necrosis factor receptor-associated factor 6 is required to inhibit foreign body giant cell formation and activate osteoclasts under inflammatory and infectious conditions. J. Bone Miner. Metab. 1–12. https://doi.org/10.1007/s00774-017-0890-z.

Pegoraro, G., Eaton, B.P., Ulrich, R.L., Lane, D.J., Ojeda, J.F., Bavari, S., DeShazer, D., Panchal, R.G., 2014. A high-content imaging assay for the quantification of the Burkholderia pseudomallei induced multinucleated giant cell (MNGC) phenotype in murine macrophages. BMC Microbiol. 14, 98. https://doi.org/10.1186/1471-2180-14-98.

Rivollier, A., Mazzorana, M., Tebib, J., Piperno, M., Aitsiselmi, T., Rabourdin-Combe, C., Jurdic, P., Servet-Delprat, C., 2004. Immature dendritic cell transdifferentiation into osteoclasts: a novel pathway sustained by the rheumatoid arthritis microenvironment. Blood 104, 4029–4037. https://doi.org/10.1182/blood-2004-01-0041.

Schlesinger, L., Musson, R.A., Johnston, R.B., 1984. Functional and biochemical studies of multinucleated giant cells derived from the culture of human monocytes. J. Exp. Med. 159, 1289–1294. https://doi.org/10.1084/jem.159.4.1289.

Seitzer, U., Scheel-Toellner, D., Toellner, K., Reiling, N., Haas, H., Galle, J., Gerdes, J., 1997. Properties of multinucleated giant cells in a new in vitro model for human granuloma formation. J. Pathol. 182, 99–105. https://doi.org/10.1002/(SICI)1096-9896(199705)182:1<99::AID-PATH807>3.0.CO;2-X.

Sheikh, F., Dickensheets, H., Pedras-Vasconcelos, J., Ramalingam, T., Helming, L., Gordon, S., Donnelly, R.P., 2015. The interleukin-13 receptor-α1 chain is essential for induction of the alternative macrophage activation pathway by IL-13 but not IL-4. J. Innate Immun. 7, 494–505. https://doi.org/10.1159/000376579.

Sissons, J.R., Peschon, J.J., Schmitz, F., Suen, R., Gilchrist, M., Aderem, A., 2012. Cutting edge: MicroRNA regulation of macrophage fusion into multinucleated giant cells. J. Immunol. 189, 23–27. https://doi.org/10.4049/jimmunol.1102477.

Skokos, E.A., Charokopos, A., Khan, K., Wanjala, J., Kyriakides, T.R., 2011. Lack of TNF-α–induced MMP-9 production and abnormal E-Cadherin redistribution associated with compromised fusion in MCP-1–null macrophages. Am. J. Pathol. 178, 2311–2321. https://doi.org/10.1016/j.ajpath.2011.01.045.

Solari, F., Domenget, C., Gire, V., Woods, C., Lazarides, E., Rousset, B., Jurdic, P., 1995.

Multinucleated cells can continuously generate mononucleated cells in the absence of mitosis: a study of cells of the avian osteoclast lineage. J. Cell. Sci. 108, 3233–3241.
Tambuyzer, B.R., Nouwen, E.J., 2005. Inhibition of microglia multinucleated giant cell formation and induction of differentiation by GM-CSF using a porcine in vitro model. Cytokine 31, 270–279. https://doi.org/10.1016/j.cyto.2005.05.006.
Tezuka, K., Sato, T., Kamioka, H., Nijweide, P.J., Tanaka, K., Matsuo, T., Ohta, M., Kurihara, N., Hakeda, Y., Kumegawa, M., 1992. Identification of osteopontin in isolated rabbit osteoclasts. Biochem. Biophys. Res. Commun. 186, 911–917. https://doi.org/10.1016/0006-291X(92)90832-6.
Trout, K.L., Jessop, F., Migliaccio, C.T., 2016. Macrophage and multinucleated giant cell classification. In: Otsuki, T., Yoshioka, Y., Holian, A. (Eds.), Biological Effects of Fibrous and Particulate Substances, Current Topics in Environmental Health and Preventive Medicine. Springer, Japan, Tokyo, pp. 1–26. https://doi.org/10.1007/978-4-431-55732-6_1.
Vignery, A., Niven-Fairchild, T., Shepard, M.H., 1990. Recombinant murine interferon-γ inhibits the fusion of mouse alveolar macrophages in vitro but stimulates the formation of osteoclastlike cells on implanted syngeneic bone particles in mice in vivo. J. Bone Miner. Res. 5, 637–644. https://doi.org/10.1002/jbmr.5650050613.
Wang, H.-Y., Jia, H.-R., Lu, X., Chen, B., Zhou, G., He, N., Chen, Z., Wu, F.-G., 2015. Imaging plasma membranes without cellular internalization: multisite membrane anchoring reagents based on glycol chitosan derivatives. J. Mater. Chem. B Mater. Biol. Med. 3, 6165–6173. https://doi.org/10.1039/C5TB00930H.
Warfel, A.H., 1978. Macrophage fusion and multinucleated giant cell formation, surface morphology. Exp. Mol. Pathol. 28, 163–176. https://doi.org/10.1016/0014-4800(78)90049-7.
Xu, M., Song, Z.-G., Xu, C.-X., Rong, G.-H., Fan, K.-X., Chen, J.-Y., Zhang, W., Jia, J.-P., Han, G., Wang, W., Chai, W., Liang, W.-T., Bi, W.-Z., Wang, Y., 2013. IL-17A stimulates the progression of giant cell tumors of bone. Clin. Cancer Res. 19, 4697–4705. https://doi.org/10.1158/1078-0432.CCR-13-0251.
Xu, Y., Zhan, Y., Lew, A.M., Naik, S.H., Kershaw, M.H., 2007. Differential development of murine dendritic cells by GM-CSF versus Flt3 ligand has implications for inflammation and trafficking. J. Immunol. 179, 7577–7584. https://doi.org/10.4049/jimmunol.179.11.7577.
Yagi, M., Miyamoto, T., Sawatani, Y., Iwamoto, K., Hosogane, N., Fujita, N., Morita, K., Ninomiya, K., Suzuki, T., Miyamoto, K., Oike, Y., Takeya, M., Toyama, Y., Suda, T., 2005. DC-STAMP is essential for cell–cell fusion in osteoclasts and foreign body giant cells. J. Exp. Med. 202, 345–351. https://doi.org/10.1084/jem.20050645.
Yagi, M., Ninomiya, K., Fujita, N., Suzuki, T., Iwasaki, R., Morita, K., Hosogane, N., Matsuo, K., Toyama, Y., Suda, T., Miyamoto, T., 2007. Induction of DC-STAMP by alternative activation and downstream signaling mechanisms. J. Bone Miner. Res. 22, 992–1001. https://doi.org/10.1359/jbmr.070401.
Yu, M., Qi, X., Moreno, J.L., Farber, D.L., Keegan, A.D., 2011. NF-κB signaling participates in both RANKL- and IL-4–induced macrophage fusion: receptor cross-talk leads to alterations in NF-κB pathways. J. Immunol. 187, 1797–1806. https://doi.org/10.4049/jimmunol.1002628.